

Fluid-Structure Interaction of Moving Flexible Bodies Using Overset Meshing, solids4Foam, and preCICE

Krishna Prasad Sah Sudi¹, Parees Palkar², and Chandan Bose³

¹ Aerospace Engineering, Pulchowk Campus, Institute of Engineering, Tribhuvan University

² FOSSEE, Indian Institute of Technology Bombay

³ Assistant Professor, Aerospace Engineering, College of Engineering and Physical Sciences, The University of Birmingham

June 8, 2026

Synopsis

Fluid-Structure Interaction (FSI) plays an important role in understanding the interaction between fluid flow and deformable structures. This study presents the numerical simulation of a flexible hollow cylinder subjected to fluid flow using a coupled FSI approach. OpenFOAM was used for computational fluid dynamics analysis, solids4Foam for structural analysis, and preCICE for two-way coupling between the fluid and structural solvers. An overset mesh technique was implemented to allow smooth motion of the cylinder without severe mesh distortion. Dirichlet boundary condition is used for solving velocity near around interface while Neumann boundary condition is used for solving traction or forces around interface. The simulation captured unsteady wake formation, vortex shedding, pressure variation, structural deformation, and stress distribution around the cylinder. FFT analysis of the lift coefficient and cylinder displacement was performed to determine the dominant fluid and structural vibration frequencies. The obtained Strouhal number showed good agreement with standard values for circular cylinder flow. The results demonstrate that the coupled OpenFOAM-solids4Foam-preCICE framework can effectively simulate overset FSI problems involving flexible moving bodies while maintaining stable two-way interaction between the fluid and structural domains.

Keywords: Fluid-Structure Interaction, Overset Mesh, OpenFOAM, solids4Foam, preCICE, Flexible Hollow Cylinder, FFT Analysis

1 Introduction

Fluid–Structure Interaction (FSI) refers to the coupled interaction between a fluid flow and a deformable structure, where the fluid forces influence the structural response and the structural deformation simultaneously affects the surrounding flow field. Such interactions are commonly observed in aerospace, marine, automotive, civil, and biomedical engineering applications including aircraft wings, turbine blades, offshore structures, flexible UAV components, and oscillating cylinders [1,2].

In aerospace and aerodynamic systems, flexible structures are often subjected to unsteady aerodynamic loading which can produce complex phenomena such as vortex-induced vibration (VIV), flutter, buffeting, and aeroelastic instability. Accurate prediction of these effects is important for ensuring structural safety, aerodynamic efficiency, and dynamic stability. Numerical simulation of these coupled problems becomes challenging when the structure undergoes large translational motion or deformation because conventional mesh deformation techniques may lead to poor mesh quality and numerical instability during long-duration simulations.

Overset meshing, also known as Chimera meshing, provides an effective solution for handling moving bodies in computational simulations. In this approach, separate meshes are generated for stationary and moving regions, and information is exchanged between overlapping meshes through interpolation. Unlike traditional deforming mesh approaches, overset methods allow the moving mesh to translate or rotate independently while maintaining good mesh quality and numerical robustness [3]. Because of these advantages, overset methods are widely used for simulations involving moving cylinders, rotorcraft, flapping wings, and other dynamic aerodynamic systems.

The development of open-source computational tools has significantly improved the capability to perform advanced multiphysics simulations. OpenFOAM is widely used for computational fluid dynamics (CFD), while solids4foam extends OpenFOAM capabilities toward solid mechanics and fluid–solid interaction analysis [4,5]. preCICE is an open-source coupling library that enables efficient partitioned coupling between independent solvers for multiphysics simulations [6]. Together, these tools provide a flexible framework for performing coupled FSI simulations involving moving and deformable bodies.

The present work is based on the `flexibleOversetCylinder` benchmark case, which couples the `overPimpleDyMFoam` fluid solver with the `solids4foam` structural solver using `preCICE`. The original OpenFOAM overset cylinder tutorial was developed primarily for rigid-body motion. In the present study, the case was extended to include structural flexibility, transforming it into a fully coupled fluid–structure interaction problem.

The fluid domain consists of incompressible airflow around a flexible hollow cylinder, while the structural domain is modeled as an isotropic linear elastic material. Overset mesh methodology is employed to accommodate large translational motion of the moving body without causing severe mesh distortion. Structural deformation is computed using the `linearGeometryTotalDisplacement` model available in `solids4foam` under the assumption of small-strain linear elasticity.

Coupling between the fluid and structural solvers is performed using `preCICE` through a partitioned implicit Dirichlet–Neumann coupling strategy. During each coupling time window, displacement information from the structural solver is transferred to the fluid solver, while aerodynamic force data from the fluid domain is mapped back onto the structural interface. To improve coupling stability and convergence, the IQN-ILS (Interface Quasi-Newton Inverse Least Squares) acceleration scheme is employed. Data transfer between non-matching fluid and solid interface

meshes is achieved using Radial Basis Function (RBF) interpolation methods.

The fluid equations are solved using the `overPimpleDyMFoam` solver with dynamic overset mesh capability, whereas the structural equations are solved using `solids4foam`. A first-order implicit Euler time integration scheme is used for both domains. FFT analysis is additionally performed on the lift coefficient and structural displacement responses to identify the dominant vortex shedding frequency and structural vibration frequency.

During implementation, compatibility issues were encountered because the original tutorial case was developed for older versions of Ubuntu, OpenFOAM, and `preCICE`. In recent software versions, mesh stretching and instability were observed near the overset outer patch during body motion. To improve mesh motion stability and avoid excessive mesh distortion, the dynamic mesh configuration was modified using: `[language=C++] dynamicFvMesh` as `dynamicOversetZoneFvMesh` and `motionSolver` as `solidBodyDisplacementLaplacian` [3]. This modification provided smoother mesh motion and improved numerical stability for the present overset FSI simulation.

The primary objective of this study is to develop a stable and efficient open-source framework for simulating fluid–structure interaction problems involving flexible moving bodies using overset mesh techniques. The developed methodology can be extended for future investigations involving aeroelasticity, vortex-induced vibration, flexible UAV structures, moving aerodynamic surfaces, and other advanced aerospace multiphysics applications.

2 Methodology

2.1 Geometry

The present study investigates the fluid–structure interaction behavior of a moving flexible body using overset meshing techniques 1. The computational configuration is based on the `flexibleOversetCylinder` benchmark case, where a deformable ring is placed inside a two-dimensional fluid domain subjected to incoming airflow. The fluid domain consists of a stationary background mesh combined with a moving overset mesh surrounding the flexible body. This overset mesh arrangement enables large translational motion of the body without causing excessive mesh distortion. The deformable structure is modeled as an elastic ring with an outer diameter of 1 m and an inner diameter of 0.5 m. The overset mesh region enclosing the cylinder moves according to prescribed oscillatory motion, while interpolation between overlapping grids ensures communication between the moving and stationary mesh regions.

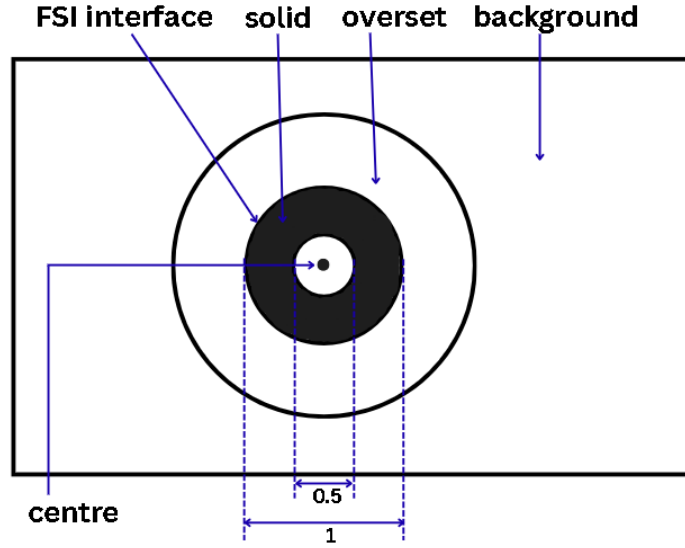


Figure 1: Geometry, unit in m

2.2 Overset Mesh

Structured, body-fitted meshes were generated for both the fluid and solid domains. In the fluid domain, mesh refinement was applied near the cylinder surface to accurately resolve the boundary layer and wake flow. A target wall resolution of $y^+ \approx 30$ was achieved using a first-layer thickness of approximately 2.34×10^{-3} m. The solid domain was discretized using finite-volume cells suitable for structural deformation analysis in *solids4Foam* 2b. Particular attention was given to the mesh resolution along the fluid-solid interface to ensure accurate transfer of forces and displacements through the radial basis function (RBF) interpolation mapping employed by *preCICE*. In the fluid solver, a moving overset mesh surrounding the cylinder overlapped a stationary background mesh, enabling large body motions while maintaining mesh quality 2a. Flow variables were exchanged between the overset and background meshes through overset interpolation throughout the simulation.

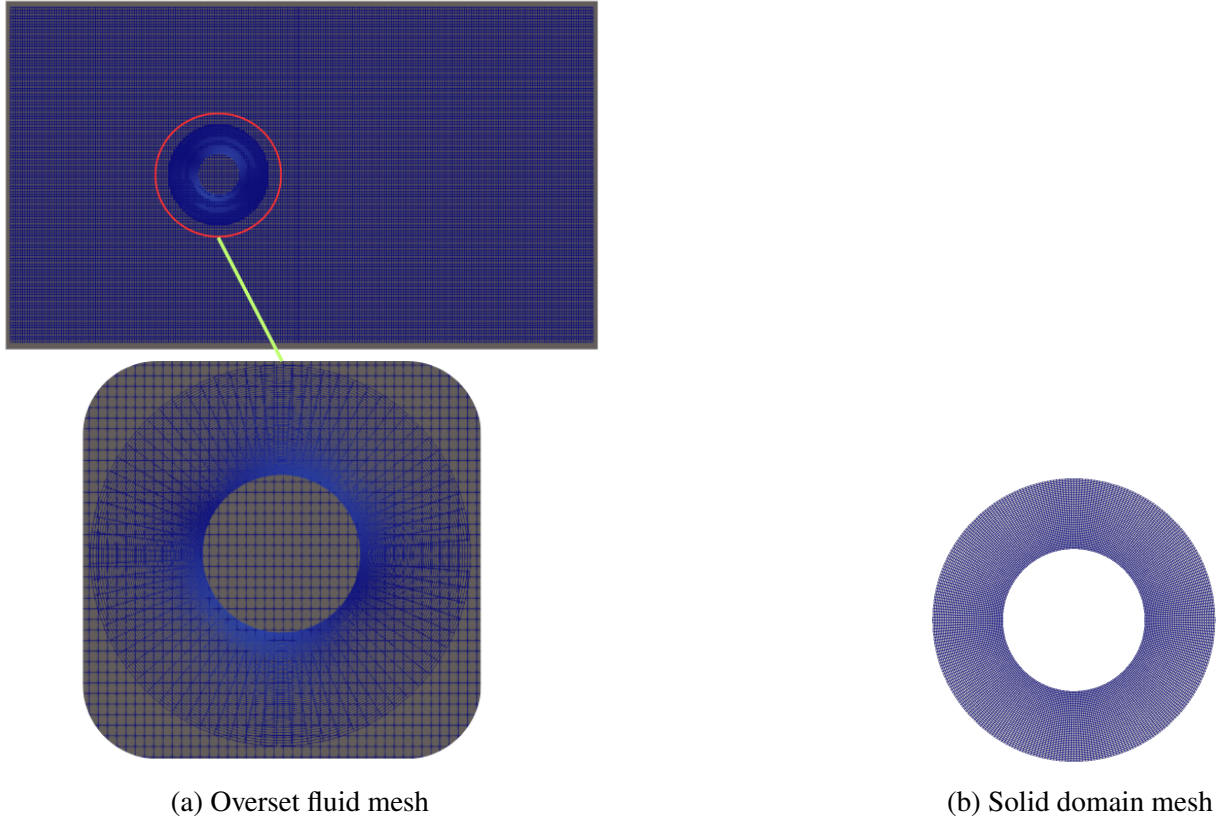


Figure 2: Computational meshes used for the fluid and solid domains.

2.3 Theory

Fluid, solid, and the interface between them are governed by three sets of equations.

2.3.1 Fluid

The fluid flow is modeled as incompressible and turbulent. The governing equations are the incompressible Navier-Stokes equations consisting of the continuity equation and momentum equation.

The continuity equation is given by:

$$\nabla \cdot \mathbf{U} = 0 \quad (1)$$

The momentum equation is expressed as:

$$\frac{\partial \mathbf{U}}{\partial t} + (\mathbf{U} \cdot \nabla) \mathbf{U} = -\frac{1}{\rho} \nabla p + \nu \nabla^2 \mathbf{U} \quad (2)$$

where \mathbf{U} is the velocity vector, p is pressure, ρ is fluid density, and ν is kinematic viscosity.

The fluid equations are solved using the overPimpleDyMFoam solver with dynamic overset mesh capability in OpenFOAM.

2.3.2 Solid

The deformable solid is modeled as a linear elastic material assuming small strains. The structural response is solved using the `linearGeometryTotalDisplacement` model available in `solids4Foam`.

The governing momentum equation for the solid domain is:

$$\rho_s \frac{\partial^2 \mathbf{D}}{\partial t^2} = \nabla \cdot \boldsymbol{\sigma} + \mathbf{f} \quad (3)$$

where \mathbf{D} represents displacement, $\boldsymbol{\sigma}$ is the stress tensor, and \mathbf{f} denotes body forces.

The constitutive relation for isotropic linear elasticity follows Hooke's law:

$$\boldsymbol{\sigma} = \lambda \text{tr}(\boldsymbol{\varepsilon}) \mathbf{I} + 2\mu \boldsymbol{\varepsilon} \quad (4)$$

where λ and μ are Lamé constants and $\boldsymbol{\varepsilon}$ is the strain tensor.

2.3.3 Fluid–Solid Interface/Parallel Implicit Coupling

For the coupled FSI interface, continuity and equilibrium conditions are maintained as:

$$\mathbf{u}_{fluid} = \mathbf{u}_{solid} \quad (5)$$

$$\mathbf{v}_{fluid} = \mathbf{v}_{solid} \quad (6)$$

$$\mathbf{n} \cdot \boldsymbol{\sigma}_{fluid} = \mathbf{n} \cdot \boldsymbol{\sigma}_{solid} \quad (7)$$

where \mathbf{u} is displacement, \mathbf{v} is velocity, \mathbf{n} is the interface normal vector, and $\boldsymbol{\sigma}$ is the stress tensor.

The implicit parallel coupling iterations continue until the interface residual satisfies the convergence criterion:

$$R^{(k)} = \left\| \mathbf{u}^{(k)} - \mathbf{u}^{(k-1)} \right\| < \varepsilon \quad (8)$$

where $R^{(k)}$ is the coupling residual at iteration k , and ε is the prescribed convergence tolerance.

2.3.4 RBF Mapping

In the present simulation, Radial Basis Function (RBF) interpolation was used to transfer displacement and force data between the non-matching fluid and solid interface meshes. The coupled solution was achieved using a parallel implicit partitioned coupling approach implemented through preCICE with IQN-ILS acceleration for improved numerical stability and convergence.

The RBF interpolation for displacement transfer can be expressed as:

$$u_f(\mathbf{x}) = \sum_{j=1}^N w_j \phi(\|\mathbf{x} - \mathbf{x}_j\|) \quad (9)$$

where u_f is the interpolated displacement at the fluid interface point, w_j are the interpolation weights, ϕ is the radial basis function, and \mathbf{x}_j represents the solid interface control points.

Similarly, force transfer between the interfaces satisfies:

$$F_s = H^T F_f \quad (10)$$

where F_f and F_s are the fluid and solid interface force vectors, and H is the interpolation matrix obtained from the RBF mapping.

2.3.5 FSI Coupling

Coupling between the fluid and solid solvers is achieved using preCICE. A partitioned Dirichlet–Neumann coupling strategy is employed, where displacement data is transferred from the structural solver to the fluid solver, while fluid force data is transferred back to the solid solver.

To improve convergence and numerical stability, the IQN-ILS quasi-Newton acceleration scheme is used. Data transfer between non-matching fluid and solid meshes is performed using radial basis function (RBF) interpolation.

The coupling procedure during each time step consists of:

- i. Solving structural deformation
- ii. Sending displacement data to the fluid solver
- iii. Updating overset mesh motion
- iv. Solving fluid flow equations
- v. Computing interface forces
- vi. Transferring forces back to the solid solver
- vii. Iterating until coupling convergence is achieved

A time step of 0.001 s is used for both solvers.

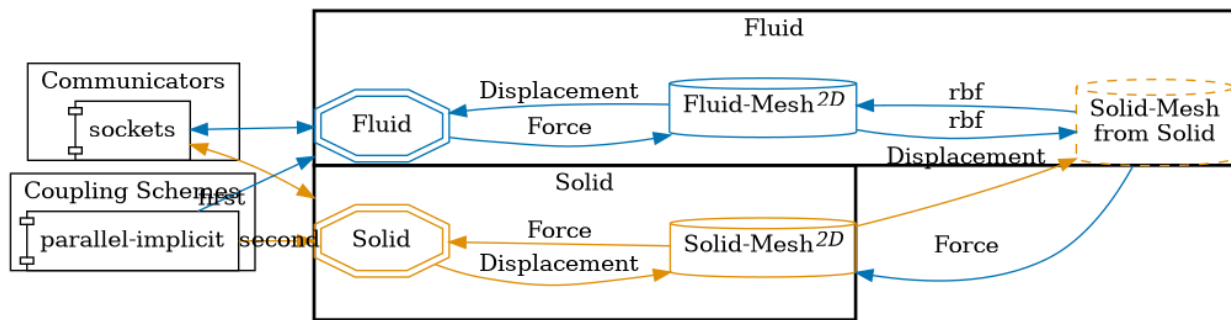


Figure 3: Flow chart of FSI

2.4 Solver Setup

2.4.1 Fluid Setup

The fluid domain is solved using the `overPimpleDyMFoam` solver available in OpenFOAM v2212. Dynamic overset meshing is employed to simulate the motion of the deformable body. Air enters the inlet boundary with a uniform velocity of 10 m/s, while pressure outlet conditions are applied at the outlet boundary. Turbulence effects are modeled using the $k-\epsilon$ turbulence model. The overset mesh surrounding the body undergoes oscillatory motion defined using `oscillatingLinearMotion`. The imposed motion consists of a harmonic displacement with an amplitude of (0.2 0.2 0) in both the horizontal and vertical directions, and an angular frequency of 3.14159 rad/s.

The first-order implicit Euler scheme is used for temporal discretization, while spatial discretization is performed using second-order finite volume methods.

2.4.1.1 Initial and Boundary Conditions

Table 1: Boundary Conditions for Fluid Domain

Patch	Velocity (U)	Pressure (p)
overset	overset	overset
walls(interface)	movingWallVelocity	zeroGradient
inlet	fixedValue	zeroGradient
outlet	inletOutlet	fixedValue
topAndBottom	zeroGradient	zeroGradient

2.4.1.2 Fluid Properties

The fluid properties used in the simulation are summarized in Table 2.

Table 2: Fluid properties

Property	Value
Density (ρ)	1 kg/m ³
Kinematic viscosity (ν)	1.48×10^{-5} m ² /s
Inlet velocity	10 m/s

2.4.1.3 Finite Volume Schemes

Different operations along with appropriate schemes are tabulated in table 3.

Table 3: Finite Volume Schemes Used in the Present Simulation

Operation	Scheme
Time Derivative	Euler
Gradient	Gauss linear
Divergence	default none; div(phi,U) Gauss limitedLinearV 1 div(phi,k) Gauss limitedLinear 1 div(phi,epsilon) Gauss limitedLinear 1 div(phi,R) Gauss limitedLinear 1 div(phi,omega) Gauss limitedLinear 1 div((nuEff*dev2(T(grad(U)))) Gauss linear
Laplacian	Gauss linear corrected
Surface Normal Gradient	corrected
Interpolation	linear
Overset Interpolation	inverseDistance

2.4.1.4 Solution Method and Control

Different fluid parameter with corresponding methods and controls that fitted for stable FSI simulation are tabulated in table 4.

Table 4: Solution Methods and Solver Controls

Parameter	Method / Value
Pressure Solver	PBiCGStab with DILU preconditioner
Velocity Solver	smoothSolver with symGaussSeidel smoother
Mesh Displacement Solver	PCG with DIC preconditioner
Pressure Tolerance	10^{-6}
Velocity Tolerance	10^{-6}
Mesh Displacement Tolerance	10^{-6}
Outer Correctors	1
Pressure Correctors	2
Non-Orthogonal Correctors	0
Momentum Predictor	false
Overset Flux Adjustment	true
Time Derivative Correction	true
Relaxation Factor	1.0
Overset Coupling Algorithm	PIMPLE

2.4.2 Solid Setup

The structural domain is solved using solids4Foam. The solid body is prescribed with a harmonic motion at its centre, having an amplitude of (0.2 0.2 0) and an angular frequency of 3.14159 rad/s, corresponding to the imposed overset mesh motion.

2.4.2.1 Boundary Conditions

Table 5: Boundary Conditions for Solid Domain

Patch	Displacement (D)	Force ($solidForce$)
centre	codedFixedValue	calculated
interface	solidForce	calculated
defaultFaces	empty	empty

2.4.2.2 Material Properties

The material is modeled as an isotropic elastic solid representing soft rubber-like behavior. The prescribed oscillatory displacement is applied at the inner boundary of the deformable ring.

The structural properties are summarized in Table 6.

Table 6: Solid properties

Property	Value
Young's modulus	0.2 MPa
Poisson's ratio	0.45
Material model	Linear elastic
Solid solver	linearGeometryTotalDisplacement

The imposed oscillatory displacement follows a sinusoidal motion in both horizontal and vertical directions.

2.4.2.3 Finite Volume Schemes

Operations along with schemes for solid4Foam are tabulated in table 7.

Table 7: Finite Volume Schemes for Solid Domain

Operation	Scheme
Second Time Derivative	Euler
Time Derivative	Euler
Gradient	leastSquares
Divergence	Gauss linear
Laplacian	laplacian(D,D) Gauss linear corrected fvBlockLaplacian(D) pointGaussLeastSquaresLaplacian
Surface Normal Gradient	corrected
Interpolation	linear interpolate(grad(D)) linear interpolate(sigma) linear

2.4.2.4 Solution Method and Control

Control methods in solids4Foam are tabulated in table 8.

Table 8: Solution Methods and Relaxation Factors for Solid Domain

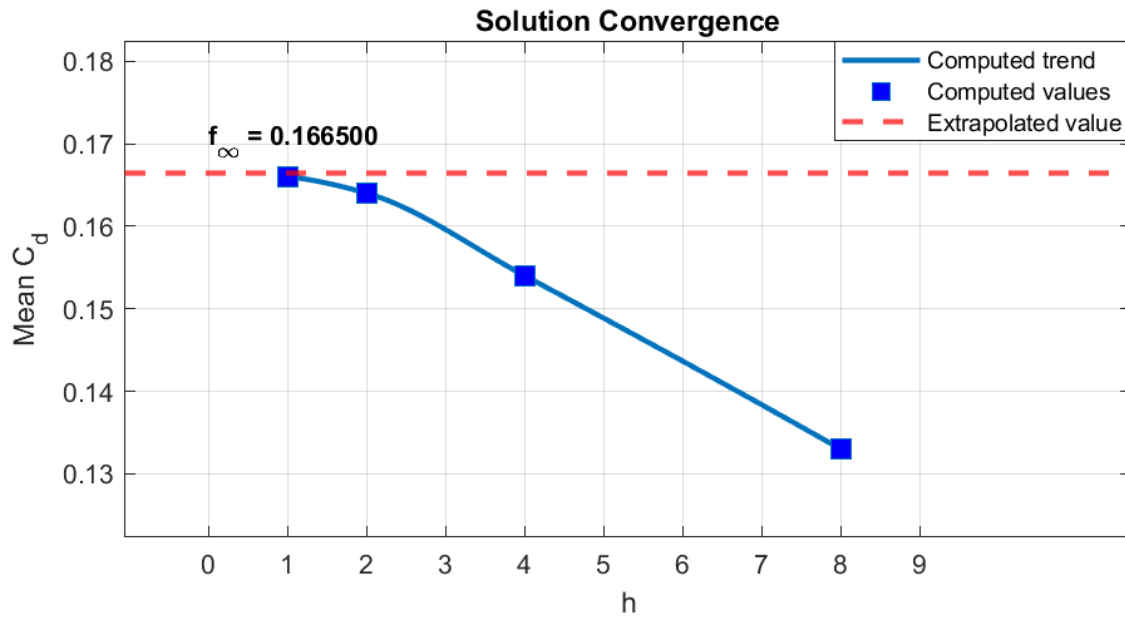
Parameter	Setting
Linear Solver	PCG
Preconditioner	FDIC
Tolerance	1×10^{-9}
Relative Tolerance	0.1
Block Solver	EigenSparseLU
Relaxation Factor for D	0.9

2.5 Verification(GCI)

A Grid Convergence Index (GCI) study is carried out in every simulation to ensure that the numerical results are not influenced by grid resolution. It is also performed to identify a mesh that balances accuracy and computational cost. Four different meshes were evaluated-coarse, medium, fine, and very fine comprising 7,950, 15,900, 31,800, and 63,600 background elements, paired with 750, 1,500, 3,000, and 6,000 overset elements, respectively. A constant grid refinement ratio of $r = 2$ was applied across successive refinement levels. The mean drag coefficient (\bar{C}_D) was chosen as the representative convergence parameter. The computed \bar{C}_D values for the coarse, medium, fine, and very fine meshes were 0.133, 0.154, 0.164, and 0.166, respectively. Using the GCI method proposed by Roache [7], the apparent order of convergence (p) was calculated iteratively (converging in 21 iterations) and found to be 2.321927. The extrapolated mean drag coefficient at infinite grid resolution was determined to be $f_\infty = 0.166500$. The asymptotic ratio of convergence was 1.012196, confirming that the solution lies well within the asymptotic convergence range and exhibits good asymptotic convergence. From the GCI study, the discretization error (GCI%) in calculating the mean drag coefficient was 4.26% for the coarse mesh, 1.91% for the medium mesh, and dropped to just 0.38% for the fine mesh, indicating that the mesh refinement was sufficient to achieve grid-independent results.

Table 9: Grid independence study including background and overset mesh elements.

Mesh	Background Elements	Overset Elements	\bar{C}_D	GCI (%)
Coarse	7950	750	0.133	4.26
Medium	15900	1500	0.154	1.91
Fine	31800	3000	0.164	0.38
Very Fine	63600	6000	0.166	-

Figure 4: h vs mean C_d

3 Results and Discussion

3.1 Displacement/Force vs Time

Figure 5 shows the variation of cylinder displacement (D_y) with time at the interface point. The displacement exhibits periodic oscillatory behavior due to the unsteady fluid forces acting on the flexible cylinder. The transverse displacement varies approximately between -0.22 m and 0.22 m, indicating the dynamic response of the structure under vortex-induced loading.

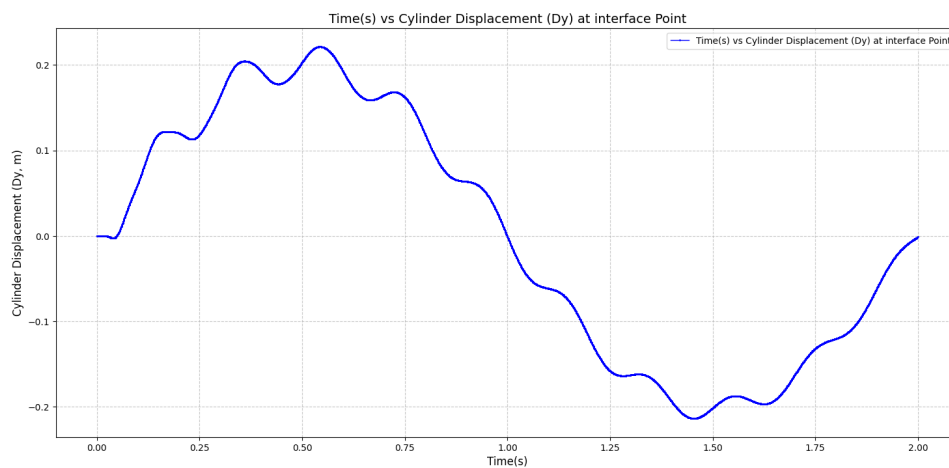


Figure 5: Time(s) vs Displacement(m)

Figure 6 presents the variation of total force in the transverse direction with time. The force fluctuates

tuates continuously because of alternating vortex shedding and fluid-structure interaction effects. The total force ranges approximately from -1.5 N to 4 N, demonstrating the unsteady aerodynamic loading experienced by the cylinder during the simulation.

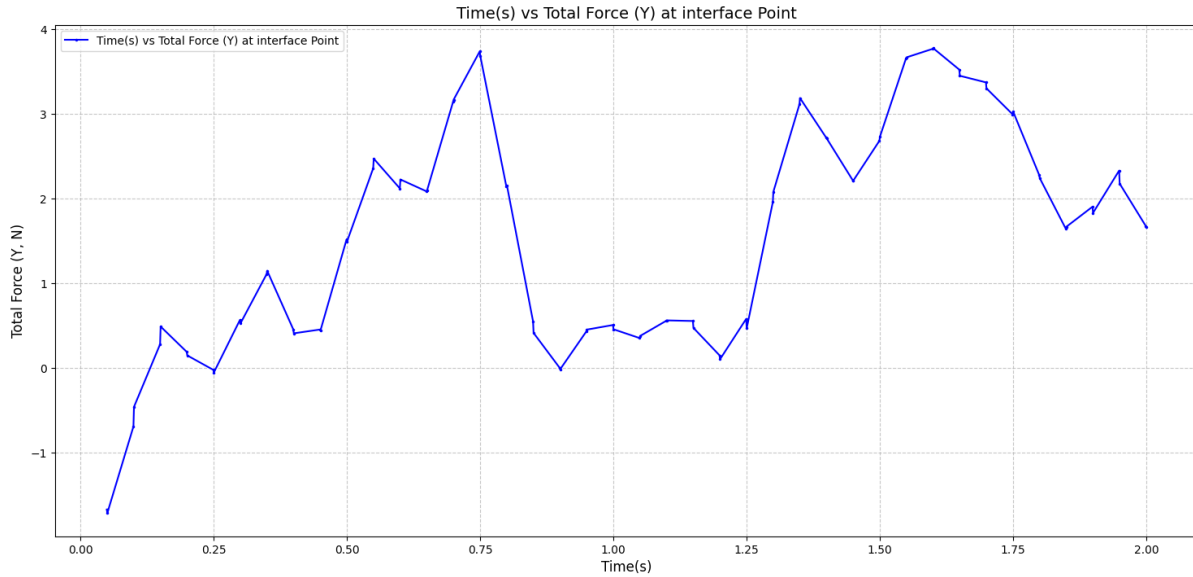


Figure 6: Time(s) vs Force(N)

3.2 Drag Coefficients vs Time

Figure 7 shows the variation of drag coefficient with time for the flexible cylinder. The drag coefficient initially increases as the flow develops around the cylinder and then exhibits periodic fluctuations due to unsteady vortex shedding in the wake region. The drag coefficient varies approximately between 0.2 and 0.8, indicating the presence of time-dependent aerodynamic forces acting on the cylinder surface.

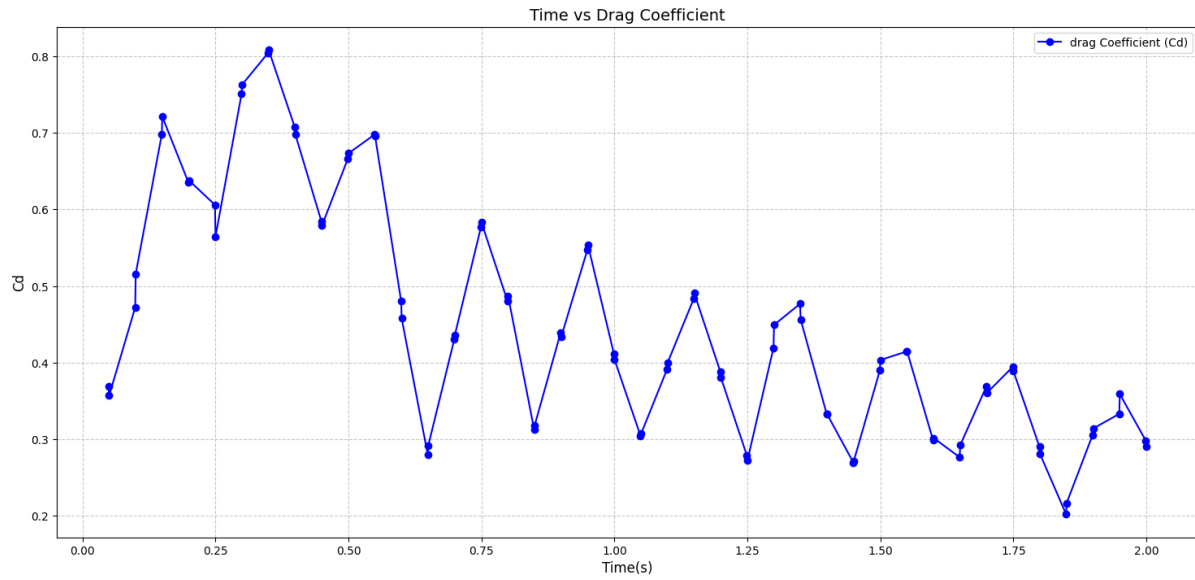


Figure 7: drag coefficient vs time

3.3 Lift Coefficients vs Time

Figure 8 presents the variation of lift coefficient with time. The lift coefficient shows oscillatory behavior caused by alternating vortex shedding behind the cylinder. These fluctuating lift forces are responsible for the transverse vibration of the flexible cylinder during fluid-structure interaction. The lift coefficient ranges approximately from -0.35 to 0.75 throughout the simulation.

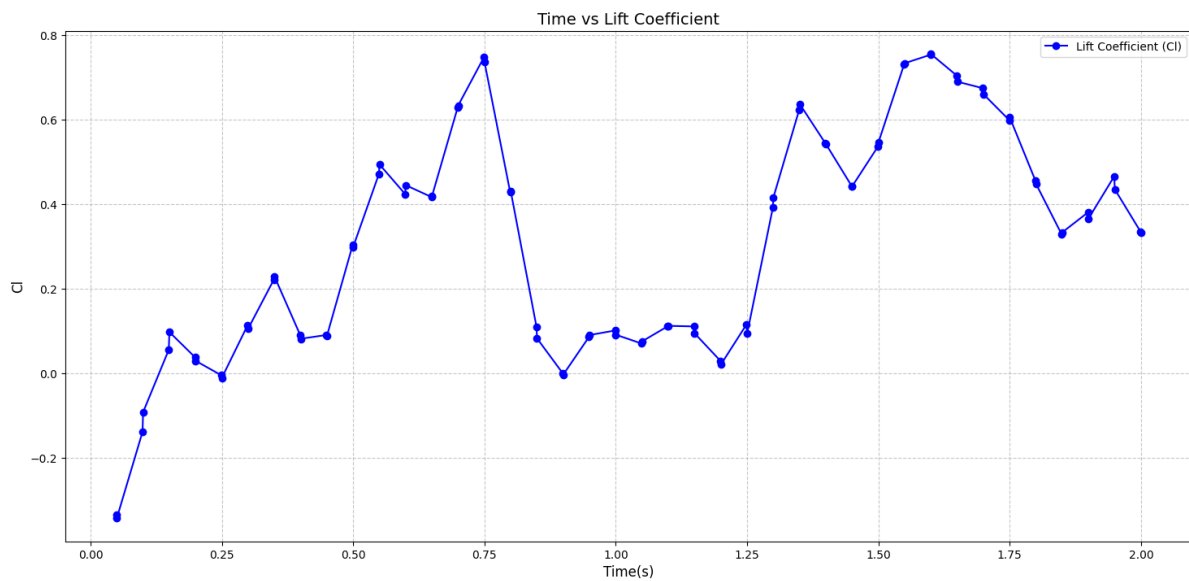


Figure 8: lift coefficient vs time

3.4 FFT of Lift Coefficients

The Fast Fourier Transform (FFT) analysis shown in Figure 9 was performed on the lift coefficient signal to determine the dominant vortex shedding frequency around the flexible cylinder. The FFT spectrum shows a clear peak at approximately 1.99 Hz, indicating the primary fluid oscillation frequency generated by periodic vortex shedding in the wake region. This unsteady wake formation produces periodic aerodynamic forces on the cylinder. The corresponding Strouhal number was found to be approximately 0.1991, which is in good agreement with the typical value for flow past a circular cylinder.

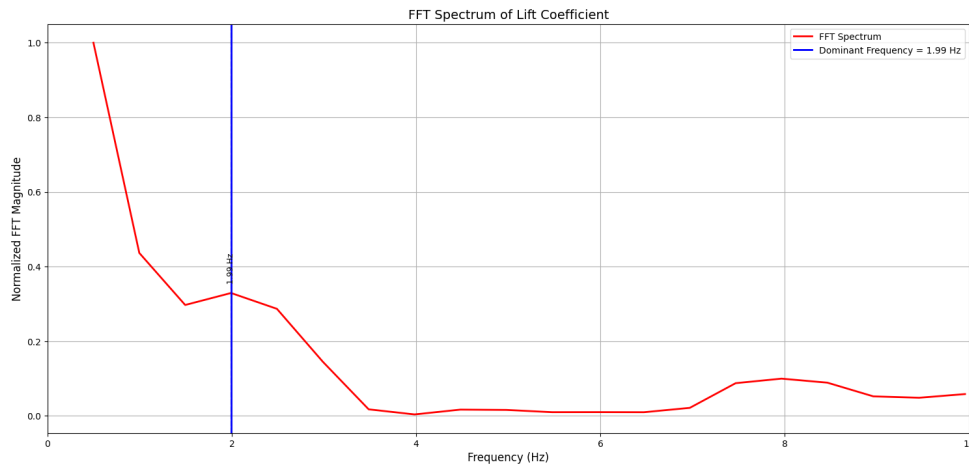


Figure 9: fft of coefficient

3.5 FFT of Displacement

FFT analysis 10 was also performed on the transverse displacement (D_y) of the cylinder to determine the dominant structural vibration frequency. The FFT spectrum indicates a dominant vibration frequency of approximately 5.00 Hz. This shows that the structural response frequency is higher than the fluid vortex shedding frequency. The difference between the fluid and structural frequencies suggests that the cylinder vibration is influenced by its structural stiffness and dynamic properties, and complete lock-in between fluid and structure has not occurred in the present simulation.

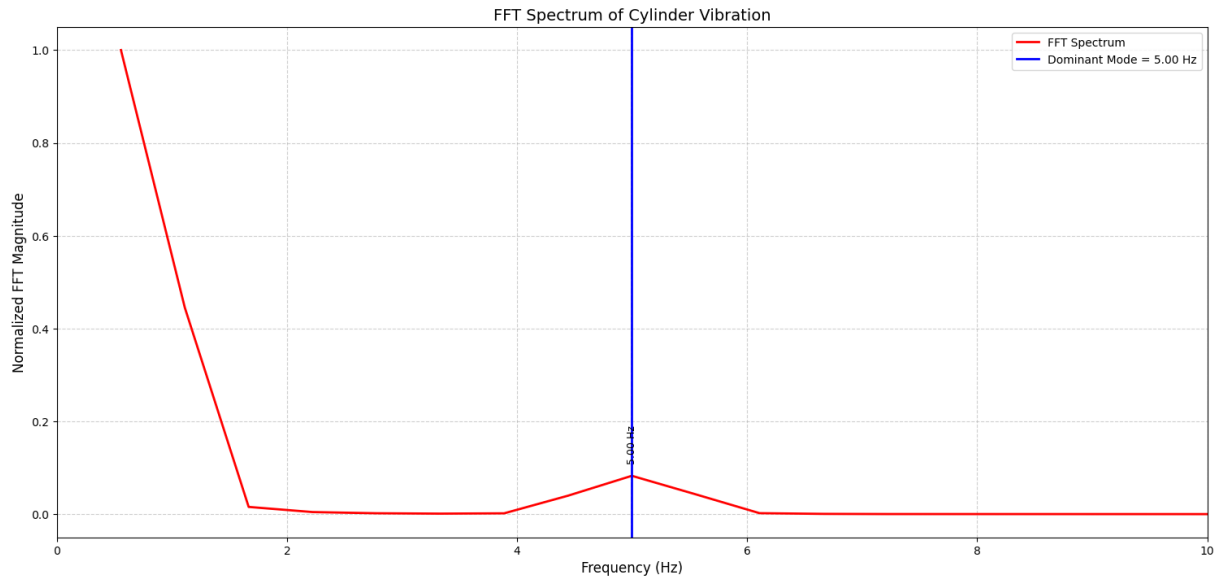


Figure 10: fft of Cylinder Vibration

3.6 Pressure Contours

Figure 11 shows the pressure contours around the flexible cylinder at different time instants. High-pressure regions are observed at the front stagnation point, while low-pressure regions develop around the separated wake behind the cylinder. The pressure distribution changes continuously with time due to vortex shedding and fluid-structure interaction effects.

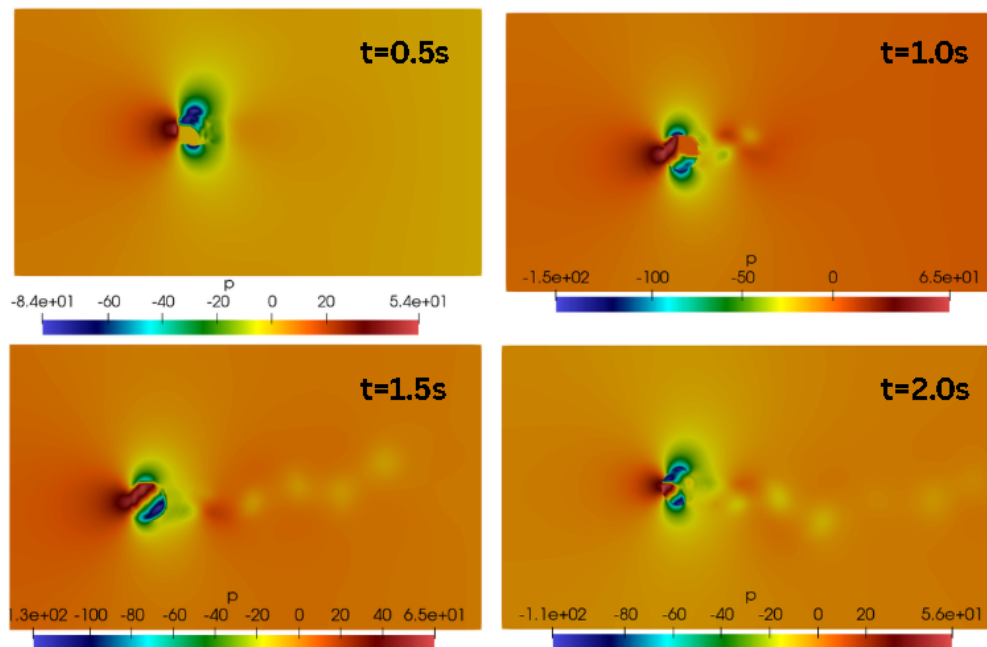


Figure 11: Pressure contours at different time

3.7 Velocity Contours

Figure 12 illustrates the velocity contours around the flexible cylinder at different time instants. The flow accelerates around the cylinder surface, while a low-velocity wake region forms behind the cylinder due to flow separation. As time progresses, alternating vortex shedding develops in the wake, producing an unsteady velocity field and demonstrating the fluid-structure interaction behavior of the system.

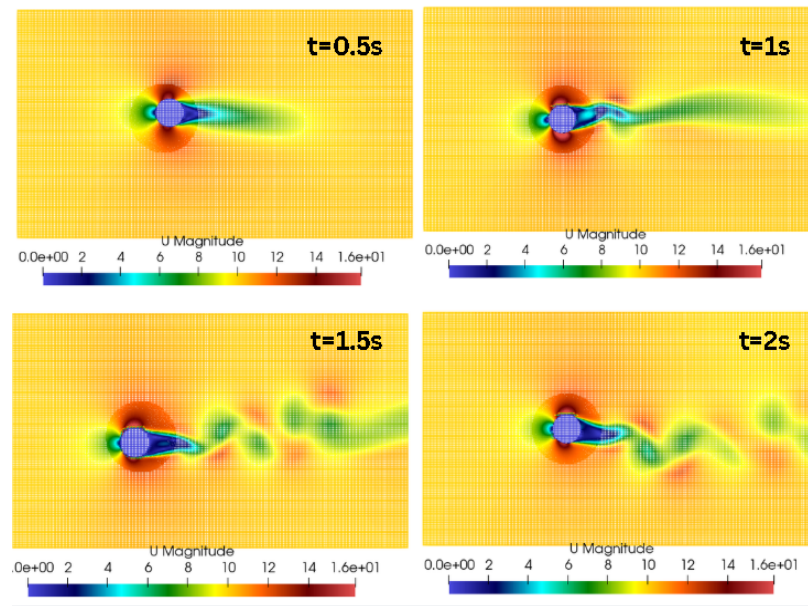


Figure 12: Velocity contours at different time

3.8 Vorticity Contours

Figure 13 presents the vorticity contours around the flexible cylinder at different time instants. Strong vorticity regions are generated near the cylinder surface due to flow separation. As time progresses, alternating vortices are shed downstream, forming a periodic wake structure known as the von Kármán vortex street. The changing vorticity pattern clearly demonstrates the unsteady flow behavior and fluid-structure interaction effects around the cylinder.

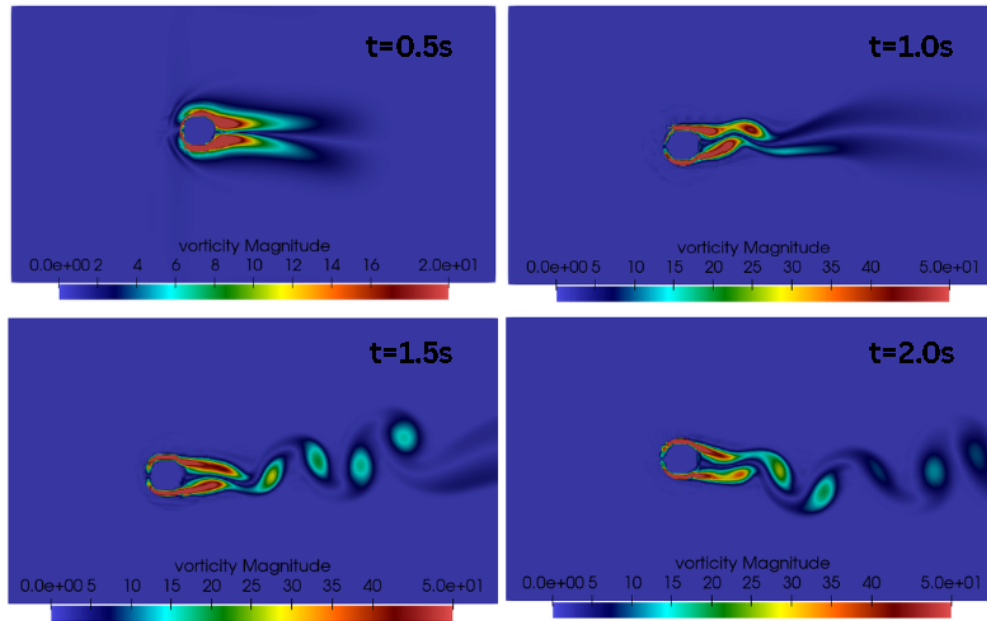


Figure 13: Vorticity contours at different time

3.9 Displacement And Stress Distribution Over hollow cylinder

Figure 15 illustrates the displacement distribution over the hollow flexible cylinder at different time instants. The cylinder undergoes continuous deformation due to the unsteady fluid forces generated by vortex shedding. Higher displacement regions are observed along the outer surface of the cylinder, indicating the dynamic structural response during fluid-structure interaction.

Figure 14 presents the stress distribution over the hollow cylinder during the simulation. The stress concentration varies with time as the aerodynamic loading changes around the cylinder surface. Higher stress regions are mainly observed near the deformed portions of the cylinder, demonstrating the effect of oscillatory fluid forces on the structural behavior.

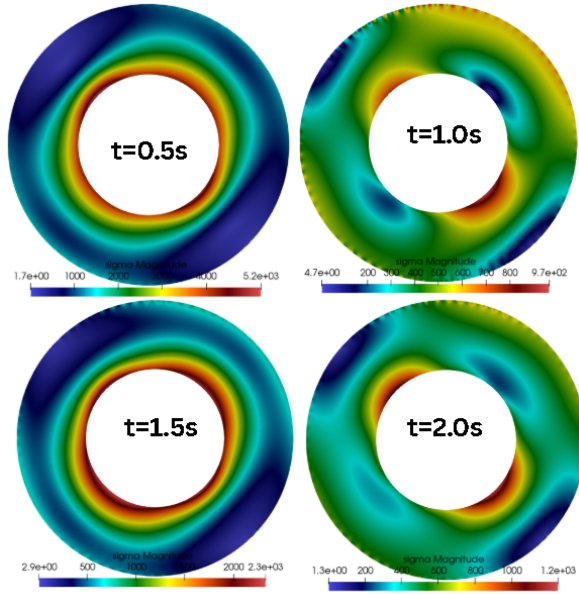


Figure 14: Stress distribution

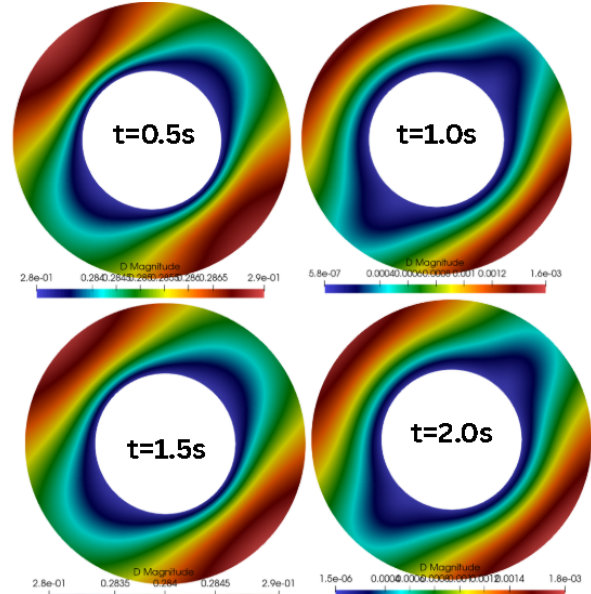


Figure 15: Displacement distribution

4 Conclusions

The coupled fluid-structure interaction (FSI) simulation successfully captured the interaction between the flexible hollow cylinder and the surrounding fluid flow using the overset mesh approach. The overset mesh moved smoothly throughout the simulation without severe mesh distortion, demonstrating the effectiveness of the method for deformable moving body simulations. The results showed periodic deformation of the flexible cylinder due to unsteady aerodynamic loading caused by vortex shedding. The pressure, velocity, and vorticity contours clearly illustrated wake development and alternating vortex formation behind the cylinder. The drag coefficient varied approximately between 0.2 and 0.8, while the lift coefficient ranged from about -0.35 to 0.75, indicating strong unsteady flow behavior and vortex-induced vibration effects. FFT analysis of the lift coefficient identified a dominant vortex shedding frequency of approximately 1.99 Hz. Using $D = 1$ m and $U = 10$ m/s, the corresponding Strouhal number was calculated as approximately 0.199, which agrees well with standard value (0.2) reported for circular cylinders. FFT analysis of the cylinder displacement showed a dominant structural vibration frequency of approximately 5 Hz. The higher structural frequency compared to the fluid shedding frequency indicates that complete lock-in did not occur during the simulation. The displacement and stress distributions further confirmed the structural response under fluid loading, with higher deformation and stress regions observed along the outer surface of the cylinder. Overall, the coupled OpenFOAM–solids4Foam–preCICE framework demonstrated stable and accurate two-way coupling performance for overset FSI simulations involving flexible moving structures.

5 Acknowledgement

I would like to express my sincere gratitude to my supervisor, Dr. Chandan Bose, for his continuous guidance, valuable suggestions, and support throughout the project. His encouragement and technical insights greatly helped in the successful completion of this work. I would also like to thank Mr. Parees Palkar (Mentor) and Mr. Yukesh Karki for their guidance, technical support, and helpful discussions during the entire project process. Finally, I would like to thank Mrs. Payel Mukherjee, the FOSSEE team, and IIT Bombay for providing the opportunity, resources, and support required to carry out this project successfully.

References

- [1] T. Richter, “A monolithic geometric multigrid solver for fluid-structure interactions in ale formulation,” *International journal for numerical methods in engineering*, vol. 104, no. 5, pp. 372–390, 2015.
- [2] B. Schott, C. Ager, and W. A. Wall, “Monolithic cut finite element–based approaches for fluid-structure interaction,” *International Journal for Numerical Methods in Engineering*, vol. 119, no. 8, pp. 757–796, 2019.
- [3] K. Ahmed, A. Hamada, L. Chatellier, and M. Fürth, “A modified overset method in open-foam ® for simultaneous motion and deformation: A case study of a flexible flapping foil,” *OpenFOAM® Journal*, vol. 4, pp. 41–61, 04 2024.
- [4] P. Cardiff, I. Batisti *et al.*, “solids4foam: A toolbox for performing solid mechanics and fluid-solid interaction simulations in openfoam,” *Journal of Open Source Software*, vol. 10, no. 108, p. 7407, 2025.
- [5] P. Cardiff, A. Karač, P. Jaeger, H. Jasak, J. Nagy, A. Ivankovic, and Z. Tukovic, “An open-source finite volume toolbox for solid mechanics and fluid-solid interaction simulations,” 08 2018.
- [6] H.-J. Bungartz, F. Lindner, B. Gatzhammer, M. Mehl, K. Scheufele, A. Shukaev, and B. Uekermann, “precice—a fully parallel library for multi-physics surface coupling,” *Computers & Fluids*, vol. 141, pp. 250–258, 2016.
- [7] P. J. Roache, *Verification and Validation in Computational Science and Engineering*. Hermosa Publishers, 1998.